This article is published as part of a themed issue of ***Photochemical & Photobiological Sciences*** of contributions from:

6th European Meeting on Solar Chemistry and Photocatalysis: Environmental Applications

Guest edited by **Josef Krysa** and **Sixto Malato**

Published in **issue 3, 2011**

Papers

Visible light induced wetting of nanostructured N–F co-doped titania films†‡

A. G. Kontos,*[a] M. Pelaez,[b] V. Likodimos,[a] N. Vaenas,[a] D. D. Dionysiou[b] and P. Falaras*[a]

Received 12th June 2010, Accepted 18th July 2010
DOI: 10.1039/c0pp00159g

Nitrogen and fluorine co-doped TiO_2 films have been prepared by dip coating of a modified titania sol–gel based on a nitrogen precursor and a nonionic fluorosurfactant as pore template and fluorine source. The modified NF–TiO_2 films absorb in the visible spectral range, between 400–510 nm and undergo reversible hydrophilic conversion under visible light to a final contact angle of 8°, in contrast to the UV limited optical response of their undoped anatase TiO_2 analogues. The phenomenon takes place at a rate slower than the corresponding one observed for the UV stimulated superhydrophilic effect. The wetting response of the N–F doped TiO_2 films correlates well with the variation of their optical properties and surface morphological characteristics and most importantly with their photocatalytic activity, rendering these materials very promising for self-cleaning applications under visible light.

Introduction

Titanium dioxide is an ideal material for photoinduced phenomena such as photocatalysis, which leads to the breakdown of organics, and superhydrophilicity resulting in high wettability.[1,2,3] Combination of the two effects leads to several applications like self-cleaning materials and antifogging surfaces. The unique photoinduced reactivity of TiO_2 stems from efficient charge separation of the photogenerated free carriers, electrons and holes. However, because of the large band gap (of about 3.0 eV) of the TiO_2 semiconductor, only UV light stimulation can excite electrons from the valence to the conduction band.

Over the past decade, strong research efforts have been undertaken in order to enable visible light induced activity of TiO_2, by doping with non-metal elements, including C, P, S and N; the last giving the most promising results,[4] probably due to interstitial nitrogen doping producing localized states that lie just above the valence band.[5] This is further supported by density functional calculations of such intragap energy states created under low temperature growth.[6] On the other hand, fluorine doping, even though it does not shift the TiO_2 band gap, causes the formation of reduced Ti^{3+} ions due to the charge compensation between F^- and Ti^{4+} as well as surface oxygen vacancies that may promote charge separation[7,8] and improve the efficiency of photoinduced processes. Co-doping with nitrogen and fluorine has been proposed as an effective means to enhance the photocatalytic activity of titania under visible light irradiation through synergistic effects between the N and F dopants that may effectively reduce the amount of oxygen defects and the concomitant electron–hole recombination that hampers the photocatalytic performance of singly doped N–TiO_2.[9–12] This synergistic approach has been exploited employing a modified sol–gel technique based on a nitrogen precursor and a nonionic fluorosurfactant. In this way structural properties of TiO_2 are tailor-designed and N–F co-doping is achieved with nitrogen and fluorine contents equal to 1.5% and 4.9%, respectively.[13] These materials are active under visible light illumination leading to the photocatalytic degradation of cyanotoxin microcystin-LR (MC-LR) pollutant in water. Very recently, the N–F doped titania was successfully immobilized in the form of thin films, preserving their visible light induced catalytic activity[14] Nevertheless, the investigation of the films' visible light induced activity is far from being complete, as modifications of the wetting properties were not examined.

Since the successful preparation of N-doped TiO_2 films, several groups have reported enhanced hydrophilicity under visible light excitation (400–530 nm);[15–18] however, very slow rates of hydrophilic conversion and final contact angles, typically above 10°, have been reached. In order to improve the photoinduced hydrophilic activity, under either visible or fluorescent (UV + visible) light irradiation, additional co-doping of a non metallic element, such as sulfur, was employed.[19,20] A similar strategy has been adopted in this work by the N–F co-doping of TiO_2 films using the template sol–gel technique and their evaluation with respect to their photoinduced hydrophilicity under UV and visible light. The presence of a significant hydrophilic character for the co-doped NF–TiO_2 films was firmly established and related to their morphological and structural characteristics.

Experimental

Control, based on undoped TiO_2, as well as NF–TiO_2 materials have been prepared by the sol–gel technique.[13] The two materials have been prepared in the same manner, apart from the addition of the surfactant and ethylenediamine in the modified sol. After preparation, the sols were left to mature for 72 h and then coated on borosilicate glass (Micro slide, Gold Seal), by dipping in and pulling out the substrate from the sol, at a withdrawal rate of 12.5 ± 0.3 cm min^{-1}. After coating, the films were dried under an infrared lamp for 20 min and calcined at 400 °C for 30 min in air atmosphere.

[a]*Institute of Physical Chemistry, NCSR Demokritos, 15310, Aghia Paraskevi, Attiki, Greece. E-mail: akontos@chem.demokritos.gr, papi@chem.demokritos.gr*
[b]*Department of Civil and Environmental Engineering, University of Cincinnati, Cincinnati, Ohio, 45221-0071, USA*

† This paper is published as part of the themed issue of contributions from the 6th European Meeting on Solar Chemistry and Photocatalysis: Environmental Applications held in Prague, Czech Republic, June 2010.

‡ Electronic supplementary information (ESI) available: Emission spectra of the light sources (Fig. S1). See DOI: 10.1039/c0pp00159g

The surface morphology, roughness and geometric surface area of the titania films were examined with a digital Instruments Nanoscope III atomic force microscope (AFM), operating in the tapping mode. Diffuse reflectance and transmittance measurements were carried out in the range of 300–800 nm employing a Hitachi 3010 spectrophotometer equipped with a 60 mm diameter integrating sphere.

The hydrophilic character of TiO_2 thin films was evaluated by examining the advancing contact angle between the thin films and deionized water droplets, as a function of the illumination time. Measurements were performed using the Contact Angle Meter (CAM) 100, KSV Instruments, Ltd., equipped with a horizontal microscope and a protractor eyepiece. Each reported value was taken as the mean one of 4–5 measurements performed at different areas of the samples. Values are recorded just after the deposition of a water droplet on the sample. After each set of measurements, the samples were purged under nitrogen gas stream.

Illumination of the films was performed with both UV and visible light lamp sources, inside a special chamber (black box) with two fans for heating management. UV irradiation was carried out using UV black-light blue lamps (Sylvania 15W/T8) with maximum wavelength output at 365 nm. The power density at the sample surface was about 0.5 mW cm^{-2}, typical for outdoor applications or conditions. For the visible light irradiation, the UV lamps were replaced by four visible light fluorescence lamps (TLD 15W/54), in combination with a 430 nm cut-off filter, resulting in wavelength output from 430 to 700 nm. In this case, the power density on the sample surface was estimated to be about 3 mW cm^{-2}. These illumination conditions simulate, in a very approximate way, the visible light solar spectrum. Alternatively, a set of 9 high power Luxeon dimmable light emitting diodes (LEDs) emitting at the narrow royal blue spectral region, in between 440 and 460 nm, where the NF–TiO_2 films present significant absorption, was used as source for visible light irradiation. The LED modulus produces a homogenous beam with a high power density of 7 mW cm^{-2} on the films. The normalized spectral power distribution of the various light sources is shown in Fig. S1 in the ESI.‡ Contact angle recovery experiments were carried out immediately after the completion of the photoinduced wetting experiments by storing samples in the dark, under ambient conditions.

Results and discussion

(1) Characterization of the films

Diffuse reflectance (R) and transmittance (T) spectra were recorded for all samples in order to evaluate the wavelength range as well as efficiency of visible light absorption. The corresponding R and T spectra from the two samples are shown in Fig. 1, together with the absorbance (A) spectra calculated by A(%) = 100 – R(%) – T(%).

The control (undoped) TiO_2 films are essentially transparent in the visible range. Interference fringes are observed, both in the reflectance and transmittance spectra due to the small thickness and the high homogeneity of the films. Absorbance is only observed in the UV spectral range and the absorption threshold is estimated to 385 nm (≈3.22 eV), which is characteristic for the anatase phase of the nanoparticulate films. On the other hand, the

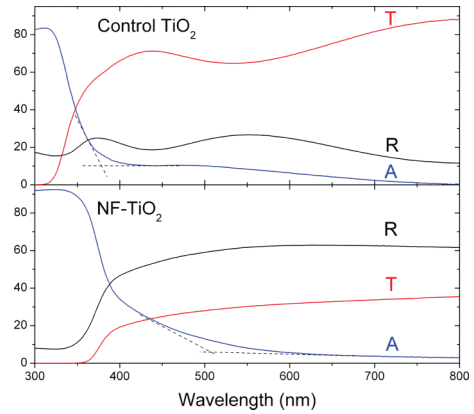

Fig. 1 Diffuse reflectance (R), transmittance (T) and calculated absorbance (A) in percentage units, for the control TiO_2 and the NF–TiO_2 films.

NF–TiO_2 films are highly reflective suggesting larger nanoparticle size and film thickness. The main absorption edge is observed at about 390 nm (≈3.18 eV), while much weaker, though clear, absorption is observed in the visible range. Assuming that this band results from a secondary modified state of the system, its absorption edge can be estimated at about 510 nm (2.43 eV), by the intersection point of the tangentials of the absorbance curve at the absorbance edge, as shown in Fig. 1. Similar strong shifts of the TiO_2 band gap have been observed in nitrogen-doped titania materials prepared with different method.[5] EPR spectroscopy has identified the characteristic paramagnetic centers arising from N dopants that form localized states above the TiO_2 valence band in the NF–TiO_2 materials.[14]

Characteristic AFM images in 9 × 9 μm surface areas of the films are shown in Fig. 2. The control TiO_2 films present a quite smooth surface characterized by a z range of a few nanometres and low roughness. In contrast, the AFM images of the NF–TiO_2 films are characteristic of rough and porous surfaces. The pore size varies from small pores with a few hundred nm in diameter to craters with diameters reaching 3000 nm. Section analysis shows that the step between the top surface and the bottom of the pores is high, between 350 to 400 nm. This justifies the high roughness of the NF–TiO_2 films that is estimated by the AFM analysis in Table 1,

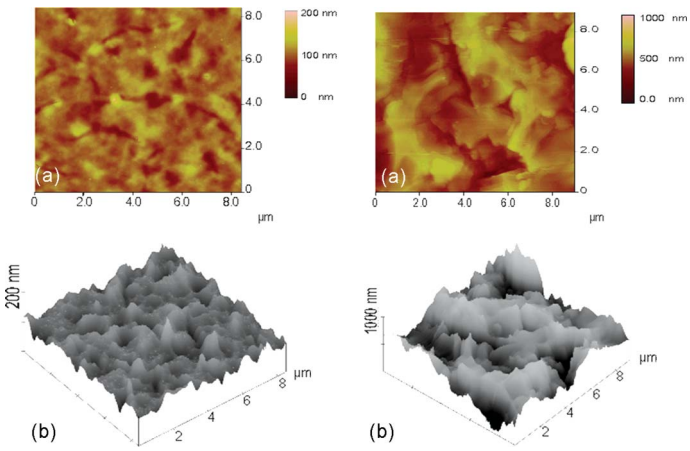

Fig. 2 AFM images of control TiO_2 (left) and NF–TiO_2 (right) samples. (a) 2D images in 9 × 9 μm areas; (b) corresponding 3D images.

Table 1 AFM calculated roughness parameters for the various samples

	Control TiO_2	NF–TiO_2
RMS/nm	13	130
R_a/nm	10	100
r	1.01	1.22

while the *z* range on large homogenous areas is very low. The above characteristics are parameterized by the root mean square (RMS) and average roughness (R_a) as well as the geometric roughness factor (r), defined as the ratio of the geometric to the projected surface area. Results are presented in Table 1.

(2) UV and visible photoinduced wetting properties

Results of UV induced superhydrophilicity are shown in Fig. 3. The samples present clear differences in their wetting behavior and sharp reduction of their contact angles upon increasing the irradiation time. The UV induced wetting of the NF–TiO_2 films is more pronounced, showing relatively lower initial contact angles and a rapid transition to the superhydrophilic state in comparison to the control samples exhibiting the largest initial contact angle and a slow rate of reduction upon UV irradiation to a saturated value of about 5°. By plotting the data on a logarithmic time scale (see inset Fig. 3), a separation of wetting stages is revealed.[21] This indicates modifications of the water/solid interfaces at contact angles equal to 40° and 20° for the control and the N–F doped TiO_2 films, respectively. The reason of the first wetting stage is not yet known, however it may be related to the adsorption of hydrophobic organic contaminants.[22] The enhanced hydrophilic activity under UV irradiation of the N–F doped relative to the undoped TiO_2 films resembles closely the trend of the UV photocatalytic degradation of MC-LR pollutants[14] and can be attributed to the increased roughness and porosity of the modified materials.

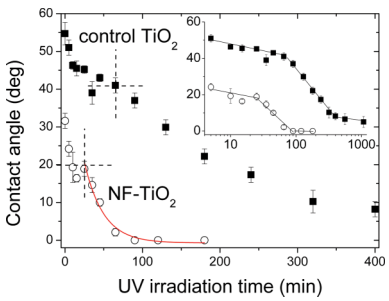

Fig. 3 Water contact angle of control TiO_2 and NF–TiO_2 films *vs.* UV (365 nm) illumination time. Solid line represents fitted first order exponential decay. Inset: Corresponding data in logarithmic full time scale, where two wetting stages are evident.

Upon illumination of the samples with visible light by either fluorescent broad-band visible light (430–700 nm) or high-power narrow-band LEDs (440–460 nm), for a period of up to 14 days, a reduction of the water contact angle on both (control and NF–TiO_2) films was observed, but hydrophilicity proceeded very slowly. The time dependence of contact angles under visible irradiation is shown in Fig. 4. The high power LED source results in faster wetting kinetics, though the superhydrophilic state is not reached in any case. Nevertheless, the NF–TiO_2 films clearly outperform with the contact angle saturating at 8° in comparison with the control sample, where a final value of 40° is reached. It is important to notice that the control films reach the end of the first wetting stage with the threshold angle of 40°, while for the NF–TiO_2 films hydrophilicity is well promoted into the second wetting stage. By plotting the data in logarithmic time scale, two regions with different slopes were observed for the NF–TiO_2 samples (see inset Fig. 4), which distinguish the transition of hydrophilicity in the second wetting stage (below 20°), despite the very slow hydrophilicity kinetics. On the other side, for the reference TiO_2, only the first wetting stage (above 40°) is evidenced by a corresponding single logarithmic component.

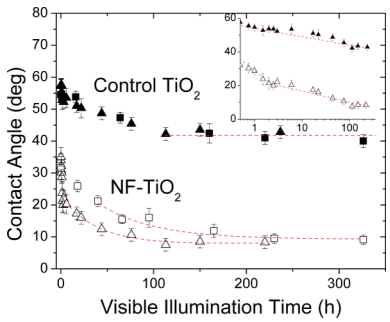

Fig. 4 Water contact angles of TiO_2 films *vs.* illumination time by visible broad (430–700 nm, square symbols) and narrow light source (440–460 nm, triangle symbols). Closed and open symbols are used for the control and the NF–TiO_2 films, respectively. NF–TiO_2 data are fitted with first order exponential decay curves. Inset: Data in logarithmic scale, where a two wetting stage behavior is evidenced only for the NF–TiO_2 films.

After becoming superhydrophilic (initial experiments), the samples are kept in the dark and examined for the 'memory' effect of superhydrophilicity by measuring the recovery of the water contact angle *vs.* time, as shown in Fig. 5. Control and aged samples recovered only partially their contact angles up to about 40° and 20°, correspondingly, *i.e.* the values that define the crossover between the first and the second wetting phases in Fig. 3. The same experiments have been carried out after the completion of the visible light excitation of the samples with the LEDs source. In this case, the contact angle of the reference sample does not change at all. On the other hand, the contact angle of the aged NF–TiO_2 recovers to 20° as also found in the case of the UV recovery measurements. Thereafter, considering the experimental uncertainties, wetting experiments are repeated with full reproducibility. A sketch of wetting behavior upon a sequence of light illumination-dark storage circles is shown in the inset of Fig. 5. The reversible wetting stage starts at θ_{in} and saturates at a lower contact angle θ_{fin}. Similar two stage wetting behavior was observed before,[16] though the reversibility of the first wetting stage was not further explored by recovery experiments.

The initial contact angles of the NF–TiO_2 films are markedly lower than those of the control ones as a result of their increased surface roughness. This indicates Wenzel's type wetting where the following relation should be valid:[23]

$$\frac{\cos\theta_{in}}{r} = \text{constant} \quad (1)$$

Using the initial contact angles θ_{in} of 40° and 20° for the control and NF–TiO_2 films, respectively, and the corresponding geometric

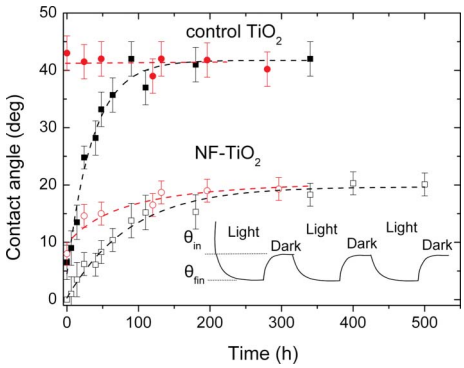

Fig. 5 Recovery of contact angle for the various films *vs.* time stored in the dark. Squares and circles mark results after completion of the UV and visible photoinduced hydrophilicity experiments, correspondingly. Solid (open) symbols represent data for control-TiO_2 (NF–TiO_2). Lines correspond to the best fit exponential growth curves. Inset: Sketch of contact angle dependence upon a sequence of light on-off circles.

roughness factors shown in Table 1, the calculated ratios of eqn (1) practically coincide for the two types of films (0.76), verifying the role of surface roughness in wetting.

The variation of contact angles between θ_{in} to θ_{fin} *vs.* time under UV or visible light irradiation has been fitted to a single exponential decay function according to eqn (2), often used for the description of the wetting kinetics.[16]

$$\theta(t) = \theta_{fin} + (\theta_{in} - \theta_{fin})\exp(-k_p t) \quad (2)$$

where k_p is the kinetic constant of the decay process. Accurate fit of the experimental data could be thus obtained with the resulting k_p values reported in Table 2.

The values of the kinetic constant have been subsequently normalized to the absorbed power density, I_a, of the films and the deduced r_p values are included in Table 2. The I_a values were obtained by integrating the spectral distribution of the incident power density I_i, as: $I_a = \int I_i(\lambda)A(\lambda)\mathrm{d}\lambda$. The imposed I_i and calculated I_a values are also given in Table 2. Comparison of the normalized kinetic constants r_p reveals that UV irradiation leads to an intense superhydrophilic conversion effect with kinetics at least two orders of magnitude faster than the corresponding ones under visible light. Distinct differences in the mechanism underlying photoinduced hydrophilicity on the NF–TiO_2 films under UV and visible illumination can be accordingly inferred. Furthermore, increasing the power density absorbed by the NF–TiO_2 samples from 0.33 (lamp source) to 1.42 mW cm^{-2} (LEDs source), results in considerable reduction of the normalized kinetic constant r_p from 0.045 to 0.018 h^{-1} (mW cm^{-2})$^{-1}$ [Table 2]. This variation implies a dependence of the photoinduced hydrophilicity on wavelength excitation, *i.e.* an $r_p(\lambda)$, that is not accounted for in our calculations.

Table 2 Recorded incident (I_i) and calculated absorbed (I_a) light power density for the various experiments on NF–TiO_2 films, together with fitted wetting kinetic constants, k_p and normalized constants per absorbed power density of the samples, r_p

Light source	I_i/mW cm^{-2}	I_a/mW cm^{-2}	k_p/h^{-1}	r_p/h^{-1} (mW cm^{-2})$^{-1}$
UV lamps 355–375 nm	0.5	0.36	2.4	6.6
Fluor. lamps 430–700 nm	3	0.33	0.015	0.045
LEDs 440–460 nm	7	1.42	0.026	0.018

The older and most accepted model of UV photoinduced superhydrophilicity relies on the hydroxylation of the TiO_2 surface induced by photo-excited holes in the material.[2] The above mechanism has been recently criticized,[24] interpreting the effect by the photocatalytic removal of carbon contamination layers, always present at the air-exposed surfaces of TiO_2. Besides, the mechanism of visible light photoinduced phenomena is even more complex. The hydrophilic and photocatalytic effects under visible light illumination are usually orders of magnitude lower than the corresponding ones under UV irradiation. This is attributed to the low hole mobility of the narrow localized states induced by nitrogen dopants[2] or the activation of only particular intra-band gap states,[16] while the role of the OH radicals is under question.

In our case, we have observed photoinduced wetting effects both under visible and UV irradiation. The control samples, apart from the initial drop of contact angle, that is not reversible, present only UV stimulated hydrophilicity and no response under visible light. On the other hand, the NF–TiO_2 films show a clear visible light induced enhancement of their hydrophilic behavior that stems from their optical absorption in the blue spectral range. Nevertheless, the wetting kinetics under visible irradiation are much slower than those observed under UV light, and a fully superhydrophilic state, with 0° contact angle, is not reached. This behavior could be explained by considering that irradiation of nitrogen-doped TiO_2 with visible light only excites electrons from the narrow localized N states above the valence band of TiO_2, where the hole mobility is very low. It is very interesting that the reaction rate for UV induced photocatalysis of MC-LR with NF–TiO_2 films is calculated to be 7×10^{-3} μM min^{-1}, which is also two orders of magnitude higher than that obtained under visible light, 4×10^{-5} μM min^{-1}.[14] These results corroborate the close interplay between photocatalysis and hydrophilicity,[24] which can be effectively combined in the design of modified titania films with self cleaning activity under solar light irradiation, a sustainable energy source.

Conclusion

Undoped TiO_2 and N–F TiO_2 films have been prepared using the self-assembly surfactant-based sol–gel method. After an initial wetting promotion the control and NF–TiO_2 films show reversible wetting with plateau contact angles of 40° and 20°, respectively. Both films exhibit superhydrophilic properties under UV irradiation. Nonetheless, only the NF–TiO_2 films absorb significantly in the blue-green spectral range (400–510 nm) and undergo slow visible light induced hydrophilic conversion, with a reduction of the wetting angle at 8°. The kinetics under visible light irradiation is two orders of magnitude less than those obtained under UV irradiation. This wetting behavior resembles closely the photocatalytic activity of NF–TiO_2 under UV and visible light indicating that co-activation of the two mechanisms could enhance the photo-induced performance of co-doped materials and permit their use in self-cleaning applications.

Acknowledgements

This work was supported by the European Commission (Clean Water project, Grant Agreement number 227017). Clean Water is a Collaborative Project co-funded by the Research DG of the European Commission within the joint RTD activities of the Environment and NMP Thematic Priorities/FP7. D.D. Dionysiou acknowledges partial funding from the U.S. National Science Foundation through a CAREER award (BES-0448117). K. Petrou is acknowledged for his assistance in AFM imaging.

References

1 A. Fujishima, T. N. Rao and D. A. Tryk, *J. Photochem. Photobiol., C*, 2000, **1**, 1.
2 K. Hashimoto, H. Irie and A. Fujishima, *Jpn. J. Appl. Phys.*, 2005, **44**, 8269.
3 H. Choi, AC. Sofranko and D. D. Dionysiou, *Adv. Funct. Mater.*, 2006, **16**, 1067.
4 R. Asahi, T Morikawa, T. Ohwaki, K. Aoki and Y. Taga, *Science*, 2001, **293**, 269.
5 A. I. Kontos, A. G. Kontos, Y. S. Raptis and P. Falaras, *Phys. Status Solidi RRL*, 2008, **2**, 83.
6 L. Tsetseris, *Phys. Rev. B: Condens. Matter Mater. Phys.*, 2010, **81**, 165205.
7 D. Li, H. Haneda, N. K. Labhsetwar, S. Hishita and N. Ohashi, *Chem. Phys. Lett.*, 2005, **401**, 579.
8 A. M. Czoska, S. Livraghi, M. Chiesa, E. Giamello, S. Agnoli, G. Granozzi, E. Finazzi, C. Di Valentin and G. Pacchioni, *J. Phys. Chem. C*, 2008, **112**, 8951.
9 D. Li, N. Ohashi, S. Hishita, T. Kolodiazhnyi and H. Haneda, *J. Solid State Chem.*, 2005, **178**, 3293.
10 D. Huang, S. Liao, J. Liu, Z. Dang and L. Petrik, *J. Photochem. Photobiol., A*, 2006, **184**, 282.
11 Y. Xie, Y. Li and X. Zhao, *J. Mol. Catal. A: Chem.*, 2007, **277**, 119.
12 C. Di Valentin, E. Finazzi, G. Pacchioni, A. Selloni, S. Livraghi, A. M. Czoska, M. C. Paganini and E. Giamello, *Chem. Mater.*, 2008, **20**, 3706.
13 M. Pelaez, A. A. De la Cruz, E. Stathatos, P. Falaras and D. D. Dionysiou, *Catal. Today*, 2009, **144**, 19.
14 M. Pelaez, P. Falaras, V. Likodimos, A. G. Kontos, A. A. De la Cruz, K. O' Shea and D. D. Dionysiou, *Appl. Catal. B*, 2010, DOI: 10.1016/j.apcatb.2010.06.017.
15 H.-Y. Chou, E.-K. Lee, J.-W. You and S.-S. Yu, *Thin Solid Films*, 2007, **516**, 189.
16 A. Borras, C. Lopez, V. Rico, F. Gracia, A. R. Gonzalez-Elipe, E. Richter, G. Battiston, R. Gerbasi, N. McSporran, G. Sauthier, E. Gyorgy and A. Figueras, *J. Phys. Chem. C*, 2007, **111**, 1801.
17 J. Premkumar, *Chem. Mater.*, 2004, **16**, 3980.
18 T. S. Ynag, -S. M-C. Yang, C-B. Shiu, W-K. Chang and M-S. Wong, *Appl. Surf. Sci.*, 2006, **252**, 3729.
19 Y. W. Sakai, K. Obata, K. Hashimoto and H. Irie, *Vacuum*, 2008, **83**, 683.
20 J. Wang, H. Li, Hongyi Li and C. Zou, *Solid State Sci.*, 2010, **12**, 490.
21 H. Fujii and H. Nakae, *Acta Mater.*, 1996, **44**, 3567.
22 K. Ozasa, S. Nemoto, Y. Li, M. Hara, M. Maeda and K. Mochitate, *Surf. Interface Anal.*, 2008, **40**, 579.
23 J. Bico, C. Marzolin and D. Quere, *Europhys. Lett.*, 1999, **47**, 220.
24 T. Zubkov, D. Stahl, T. L. Thompson, D. Panayotov, O. Diwald and J. T. Yates, Jr, *J. Phys. Chem. B*, 2005, **109**, 15454.

